Results in Engineering 28 (2025) 107679

Contents lists available at ScienceDirect

Results in Engineering

journal homepage: www.sciencedirect.com/journal/results-in-engineering

Research paper

The impact of moderate thermal fluctuations on dolomite: From strength enhancement to microstructural sensitivity

Abdel Kareem Alzo'ubi [a], Mahmoud Alneasan [b,*]

[a] Civil Engineering Department, Abu Dhabi University, Al Ain, UAE
[b] Civil Engineering Department, Latakia University, Latakia, Syria

A R T I C L E I N F O

Keywords:
Thermal cycling
Dolomite
Tensile behavior
Compressive behavior
Shear behavior
Fractures

A B S T R A C T

Understanding the long-term effects of moderate thermal cycling on dolomite is vital due to its widespread use and prevalence in civil engineering, geological, and geotechnical applications, where materials are often exposed to daily temperature fluctuations. This study investigates the behavior of dolomite subjected to up to 500 natural thermal cycles between 20 and 60 °C, providing a comprehensive assessment of the material's physical and mechanical changes. Through systematic evaluation, the research revealed that the mechanical properties of dolomite—such as tensile, compressive, and shear strengths—initially improved significantly, with respective increases of 24.28%, 31.95%, and 42.96% observed up to 350 cycles. However, a slight decline in performance followed after 500 cycles, with these strengths decreasing by 3.59%, 4.48%, and 4.98%, respectively. Parallel trends were recorded across other physical and mechanical parameters, including density, porosity, ultrasonic velocity, and elastic moduli. Notably, while chemical and phase compositions remained stable under thermal exposure up to 70 °C, microstructural shifts—particularly in void volume—exhibited pronounced sensitivity. A reduction of 72.3% in void space after 352 cycles was followed by an increase of 46.9% at 500 cycles, strongly correlating with the observed mechanical trends. These findings highlight the critical role of thermal cycling in enhancing dolomite's mechanical properties within a specific cycle range, offering valuable insights for engineering applications in thermally dynamic environments. The results are particularly relevant for infrastructure design, geothermal systems, and subsurface storage, where moderate thermal fluctuations are common, ensuring optimized material selection and long-term stability.

1. Introduction

Understanding the effects of thermal cycling on dolomite behavior at moderate temperatures (20–60 °C) is essential, as these conditions can profoundly influence the stability and durability of geological formations in both surface and subsurface environments. Dolomite, a common carbonate mineral, undergoes physical and microstructural changes under moderate thermal fluctuations, which can impact slope stability and underground structures [1,2]. At the surface, daily and seasonal temperature variations cause differential expansion and contraction, leading to microfracturing, reduced rock strength, and an increased risk of landslides. Underground, thermal cycles near geothermal zones, excavations, or ventilated tunnels can alter permeability, porosity, and strength, thereby affecting groundwater flow and structural integrity. Surface temperature changes result from solar cycles, seasons, and weather, while subsurface fluctuations originate from geothermal gradients, groundwater movement, and human activities like mining. Understanding these effects is essential for predictive modeling and risk mitigation in geological engineering, ensuring the stability of slopes, tunnels, and repositories.

Geological formations are significantly influenced by two primary thermal fields: constant and variable. A constant thermal field implies that rocks are subjected to a sustained elevated temperature. While this might not immediately induce new microcracks at moderate temperatures, prolonged exposure can lead to changes in mineralogical structure, pore fluid behavior, and overall rock strength, particularly at higher temperatures where mineral phase transformations or decomposition can occur. Extensive research was conducted to understand the effects of constant thermal fields on the mechanical properties of rocks across varying temperature ranges. Studies on thermally damaged rocks reveal distinct failure mechanisms based on mineral content. According to Chen, et al. [3], the decline in macro-mechanical properties at high

* Corresponding author.
E-mail address: mahmoud.alneasan@latakia-univ.edu.sy (M. Alneasan).

https://doi.org/10.1016/j.rineng.2025.107679
Received 25 August 2025; Received in revised form 26 September 2025; Accepted 9 October 2025
Available online 11 October 2025

temperatures results from a combination of thermal expansion, phase transformation, and decomposition. The study contrasts the behavior of two common rock types: in granite, which is rich in feldspar, and quartz-rich sandstone. In granite, damage manifests as internal mineral cracking from thermal stress, while in quartz-rich sandstone, the dominant mechanism is a temperature-induced reduction in intergranular cohesion. The work of Qiu, et al. [4] on cyclic loading indicates that higher temperatures exacerbate the decline in the bearing capacity of granite, although confining pressure provides a stabilizing effect that diminishes this temperature-dependent difference. Numerous studies have systematically investigated how sustained thermal exposure alters rock behavior under different loading conditions, including uniaxial and triaxial compression [5–7], direct and indirect tension [8,9], and shear stress regimes [10–12]. Additionally, the impact of prolonged heating on fracture initiation, growth, and coalescence was a major focus in rock mechanics literature [10,13]. These investigations highlight the critical role of temperature-dependent mineralogical changes, thermal cracking, and microstructural evolution in determining the overall mechanical response of rocks under thermal-mechanical coupling.

Variable thermal fields, such as thermal cycles, involve repeated heating and cooling. These fluctuations are far more damaging to rock properties. Rocks are composed of various minerals with different thermal expansion coefficients. During heating, minerals expand unequally, creating internal stresses at grain boundaries (intergranular microcracks) and even within individual mineral grains (intragranular microcracks). Upon cooling, the differential contraction exacerbates these stresses. Repeated cycling leads to fatigue damage, promoting the initiation and propagation of these microcracks, ultimately reducing rock strength, stiffness, and increasing permeability [14–17]. Given the growing significance of thermal fluctuations in rock mechanics and geological engineering, extensive research has explored the influence of thermal cycles across various lithologies, revealing that both rock type and test conditions critically modulate thermal damage responses. Hajpál [18] distinguished between two thermally induced crack types: "cycling cracks" arising from mismatched mineral expansion under uniform temperatures, and "thermal cracks" triggered by stress gradients in non-uniform fields. Zhang, et al. [19] observed degradation in dolomitic marble after 1000 thermal cycles. They noted that while other strength parameters, such as Uniaxial Compressive Strength (UCS), decreased immediately, the S-wave velocity initially increased before deteriorating after 400 cycles. Rong, et al. [20] linked increased cycle count to enhanced fragmentation and compromised integrity in granite and marble. At the microscale, Mo, et al. [21] recorded mineral-specific changes in modulus and hardness for quartz, plagioclase, and biotite during thermal cycling. Villarraga, et al. [22] reported reduced compressive strength and P-wave velocity in limestone under over 1000 dry cycles, while Voake, et al. [23] found tensile weakening in water-saturated chalk. Cui, et al. [24] demonstrated irreversible damage in granite under repeated thermal-water quenching, and Liu, et al. [25] identified elastic modulus shifts near the α/β phase transition of quartz, confirming that rock degradation occurs during both heating and cooling phases. Ge, et al. [26] emphasized that sandstone exhibited limited mechanical decay below 400 °C, though acoustic signals revealed progressive fracturing. Collectively, these studies illustrate the complex and lithology-dependent pathways through which thermal cycling alters rock microstructure, mechanical strength, and fracture evolution. According to Mosaddegh, et al. [27], the compressive strength of carbonate building stones changes significantly under thermal cycling. At +100 °C, the strength of travertine nearly doubled, while that of marble increased by 30 %.. However, after exposure to a higher temperature of +300 °C and repeated heating-cooling cycles, the strength of both stones decreased compared to their performance at +100 °C. Hu, et al. [28] reported that fatigue induced by cyclic thermal shock in limestone alters its calcite crystal structure. This degradation promotes crack formation at crystal boundaries, which significantly compromises the material's mechanical integrity and heat transfer properties. A decade-long study by Gasc-Barbier, et al. [29] on dolomitic limestone columns revealed that, while short-term thermal cycles induce reversible thermoelastic deformation, long-term analysis identified a significant drift in displacements. This irreversible effect suggests that the rock's behavior is governed by more complex mechanisms, such as viscoplasticity or material fatigue.

Unlike previous studies that primarily focused on granite and sandstone using rapid water-cooling methods, this research systematically investigates the long-term effects of moderate thermal cycling (20–60 °C) on dolomite, an area largely overlooked in the literature. Dolomite was selected as the target material due to its dual significance: it is a geologically abundant carbonate rock, constituting approximately30 % of sedimentary rocks, and it serves as a critical resource in civil engineering applications. Its selection is further justified by its pronounced sensitivity to thermal cycling, which induces microstructural changes such as microcracking and calcite decarbonation, making it an ideal model for studying thermo-mechanical weathering and the long-term durability of rock masses subjected to fluctuating thermal regimes typical of geothermal and subsurface engineering projects. The primary objective is to elucidate dolomite's behavior under moderate thermal cycles between 20 and 60 °C, including its responses to tension, shear, and compression. We specifically target dolomite and simulate realistic surface and subsurface environments through up to 500 gradual thermal cycles, addressing a critical gap in the literature. The methodology integrates a comprehensive, multi-scale, multi-property assessment—encompassing density, porosity, sound velocity, tensile, compressive, and shear strengths and moduli, fracture toughness, as well as detailed microstructural, chemical, and phase analyses—to provide robust insights into degradation behavior. This study offers a holistic understanding of dolomite's thermo-mechanical response under realistic thermal conditions, informing geological engineering and construction practices where fluctuating temperatures are prevalent.

2. Methods

2.1. Experimental procedure

2.1.1. Preparing rock specimens

To comprehensively investigate the impact of thermal cycles on the mechanical properties of dolomite, four distinct sample types were prepared: Brazilian discs for assessing tensile behavior, cylindrical specimens for evaluating compressive strength, semi-circular bend samples for analyzing pure mode I and II tensile fracture behavior, and short core in compression specimens for examining pure mode II shear fracture behavior.

As illustrated in Fig. 1, sample preparation began by producing prismatic specimens from a single rock block to ensure homogeneity (Fig. 1a). These prisms were then shaped into cylindrical cores (Fig. 1b) and polished with fine P600 sandpaper to achieve smooth surfaces (Fig. 1c). The cores were cut to the required lengths: 45 mm for Semi-Circular Bend (SCB) specimens, 25 mm for Brazilian discs, and 100 mm for Short Core in Compression (SCC) and cylindrical cores intended for uniaxial and triaxial compression tests. For the 100 mm cylindrical cores, end-face parallelism was maintained within 0.020 mm, and perpendicularity to the cylinder axis was kept within 0.25°, as verified using a high-precision piacolis and a dial indicator (resolution 0.001 mm), ensuring compliance withthe dimensional accuracy specified by ASTM D4543. Notably, notched SCB and SCC specimens were prepared using a 1 mm diamond-tipped blade (Fig. 1e). Fig. 1f to -j show the final prepared Brazilian discs, cylindrical samples, SCB samples, and SCC samples. All samples were equipped with strain gauges to enable precise examination of thermal cycling effects on the deformation properties of dolomite. The SCB and SCC specimens were prepared according to strict dimensions and conditions (e.g., notch length, span, and geometry) shown in Fig. 1k to -m, which are discussed in detail in Section 2.2 to establish the theoretical basis for these specimens and their role in

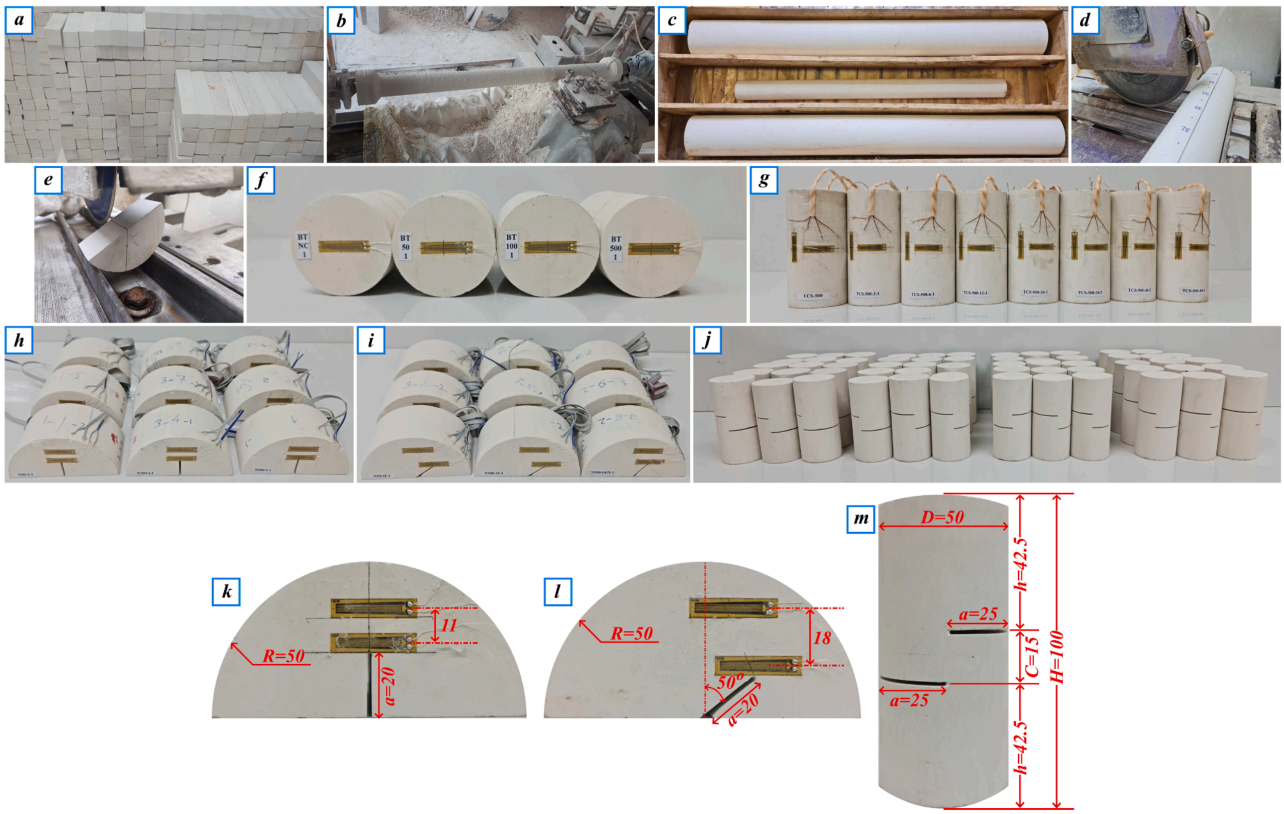

Fig. 1. Test sample preparation steps, (a) prismatic samples, (b) rotation and carving process, (c) resulting rock cores with 50 or 100 mm diameters, (d) slicing process, (e) notching process, (f) Brazilian discs, (g) cylindrical specimens, (h) pure mode I SCB specimens, (i) pure mode II SCB specimens, (j) SCC specimens, (k, l and m) geometric details of pure mode I-SCB, pure mode II-SCB and SCC specimens.

generating the tensile and shear fractures required for this study.

2.1.2. Thermal cycling

The dolomite samples underwent cyclic thermal treatment following the temperature profile illustrated in Fig. 2. The temperature variations during each thermal cycle are shown over time in the figure. To ensure uniform heat distribution, two temperature sensors and two controllers were used: one external sensor to monitor the furnace temperature and one internal sensor embedded within a sample to measure its internal temperature. These temperature sensors are PT1000 type, capable of measuring temperatures up to 500 °C with a precision of ±0.1 °C. Each sensor has dimensions of 4 × 30 mm and comes with cables and standard connectors to interface with a data logger for recording temperature versus time. The furnace was heated gradually at a controlled rate of less than 2 °C per minute to prevent thermal shock. The external sensor tracked the furnace temperature until it reached the target of 60 °C, at which point the corresponding controller stabilized the temperature. This temperature was maintained until the internal sensor also

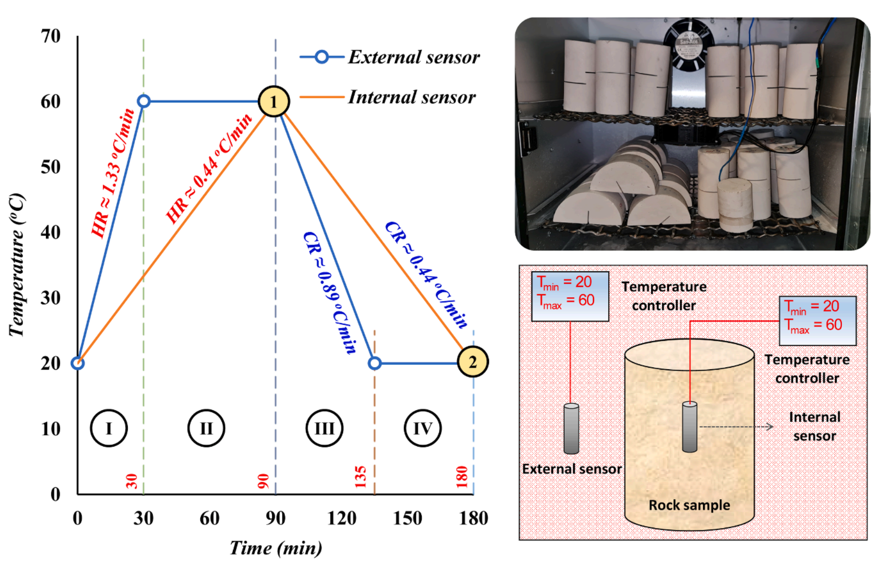

Fig. 2. Temperature variation over time during each thermal cycle.

registered 60 °C, indicating thermal equilibrium between the sample's outer and inner sections (denoted as Point 1 in Fig. 2). After reaching this first equilibrium point (Point 1), the external sensor's controller terminated heating, initiating a natural cooling phase. The external temperature was monitored until it dropped to the study's minimum threshold of 20 °C. Once reached, the ambient temperature was held constant until the sample's internal temperature equilibrated at 20 °C, marking the second thermal equilibrium point (Point 2). This completed the first thermal cycle, after which the second cycle began. Uniform heating of the samples is essential for accurately assessing thermal damage in the rock. This is achieved through a combination of equipment design and a controlled protocol. A fan-assisted oven circulates air to minimize temperature gradients within the chamber, while a slow ramp rate is employed for both heating and cooling to prevent thermal stresses and large temperature differences between the surface and the core. The gradual ramp allows heat to conduct evenly through the rock, ensuring the entire sample reaches the target temperature uniformly and reducing the risk of non-representative thermal damage. Thermal equilibrium is established and verified by the dual-sensor system described in Fig. 2.

The experimental design for thermal cycling was directly based on realistic diurnal and seasonal temperature extremes observed in arid climates such as the UAE and the Arabian Gulf, where daily and seasonal fluctuations often exceed a 40 °C range between the selected thresholds of 20 °C and 60 °C. Although a single cycle in this accelerated laboratory test does not precisely represent one full year, it provides a simplified and controlled simulation of the repeated thermal stress events that occur over time in reality. This cycle captures the critical transition between the high and low temperatures experienced by rock formations, which drive the physical processes of thermal fatigue and degradation central to the study's objectives of predicting long-term weathering and assessing risks to infrastructure. These temperature changes induce repeated thermal expansion and contraction in rock masses, leading to microcracking, fatigue, and progressive degradation of mechanical properties—processes that compromise the stability of natural slopes, foundations, and infrastructure [30]. In such environments, dolomite—a common carbonate rock—is particularly vulnerable due to its heterogeneous composition and sensitivity to thermal stress. Understanding its behavior under cyclic heating and cooling aids in predicting long-term weathering patterns, assessing risks to construction projects (e.g., roads, pipelines, and buildings), and developing mitigation strategies to enhance infrastructure resilience. Beyond arid regions, this research has broader applications in deep engineering projects where temperatures fluctuate within the 20–60 °C range, such as underground energy storage (e.g., compressed air or hydrogen), geothermal systems, and tunnel engineering. For instance, subsurface cavities in dolomite formations used for energy storage experience cyclic thermal loading during injection/extraction cycles, potentially compromising their structural integrity over time. Similarly, tunnels in carbonate-rich strata may undergo thermally induced stress redistribution, affecting long-term stability. By quantifying dolomite's response to low-temperature thermal cycles, this study provides essential data for optimizing design criteria, ensuring the durability of engineered structures, and minimizing maintenance costs in both surface and subsurface environments subjected to thermal stress.

Based on the above, the use of a 20 to 60 °C thermal cycle in our accelerated laboratory test is a controlled, simplified representation of the repeated thermal stress that rocks experience over time due to diurnal and seasonal temperature fluctuations. We acknowledge that a single cycle does not directly correspond to one full year of real-world exposure; rather, it serves as a standardized unit of thermal stress to enable direct comparison between different rock types and conditions in a laboratory setting. This methodology allows us to accelerate degradation processes and observe long-term effects within a manageable timeframe. A cycle is defined as a complete temperature swing from the low point of 20 °C to the high point of 60 °C and back to 20 °C. The number of cycles, such as 500, is not intended to represent a specific number of years but instead serves as a measure of the cumulative thermal stress applied to the specimens [31].

2.1.3. Testing procedure

Fig. 3 shows the testing device and loading configurations used in this study, which employed a GOTECH system with a 20-ton capacity, extendable to 60 tons by replacing the load cell. The device was adapted with different loading setups to perform the Brazilian Splitting Test (BST), Semi-Circular Bending Test under pure tension (SCB-I), Semi-Circular Bending Test under pure shear (SCB-II), Uniaxial Compressive Strength (UCS), Short Core in Compression under Uniaxial Loading (SCC-U), Triaxial Compressive Strength (TCS), and Short Core in Compression under Triaxial Loading (SCC-T).

For tests that consider the effect of lateral pressure—such as the TCS and SCC-T tests—experiments were conducted under three lateral pressure levels: 3, 6, and 12 MPa. Investigating how 20–60 °C thermal cycles and confining pressures within this range influence the triaxial compressive strength and shear fracture propagation in dolomite-rich rocks is vital for geological engineering and rock mechanics. These insights have significant implications for surface, subsurface, and deep rock structures. Thermal cycling induces microcrack development due to differential mineral expansion, weakening the rock and changing fracture propagation patterns—particularly under shear-dominated failure modes. This is critical for slope stability and fault reactivation. Confining pressures simulate depth-dependent stress conditions: low pressures (3 MPa) represent shallow structures like rock slopes and tunnels; intermediate pressures (6 MPa) correspond to mid-depth reservoirs and underground excavations; and high pressures (12 MPa) mimic conditions in deep mining and geothermal systems. The combined effects of thermal and mechanical loading reveal whether thermal fatigue accelerates damage or if confining pressure inhibits cracking. These factors influence fluid flow pathways in reservoirs and are essential for assessing the long-term stability of dolomite-rich formations.

All tests were carried out in strict accordance with ASTM and ISRM guidelines by fixing the piston advance at 0.2 mm/min, which corresponds to stress application rates of roughly 0.5–1.0 MPa/s for compressive (ISRM-D 2938) and 0.05–0.35 MPa/s for tensile tests (ISRM-D 3967), thereby ensuring fractures occurred within the 2–15 min and 1–10 min windows specified. A GOTECH servo-hydraulic machine maintained this displacement profile through closed-loop control: dual LVDTs supplied continuous position feedback to the servo valve, which automatically fine-tuned flow to eliminate any drift. Analysis of the resulting load–load-displacement records from all specimens confirmed unwavering velocity control and produced failure times of 2–6 min, fully satisfying the prescribed standards.

2.2. Analysis method of SCB and SCC tests

The analytical approach in this study employed two distinct specimen geometries, the Semi-Circular Bend (SCB) and the Short-Center Cracked (SCC), to investigate mode I (tensile) and mode II (shear) fracture propagation, respectively. The SCB specimen was analyzed using a three-point bending configuration, where a notched semi-circular sample was placed on two supports with a span of 2S and loaded until failure at a critical load (P_{cr}). The resulting stress intensity factors ($K_{I\text{-SCB}}$ and $K_{II\text{-SCB}}$) at the notch tip were calculated based on the specimen's specific geometry, including its radius (R), notch length (a), support span ($2S$), and notch inclination angle (β). For this analysis, specific dimensionless parameters ($a/R = 0.2$, $S/R = 0.5$) were selected to achieve pure mode loading conditions: $\beta = 0°$ for pure mode I ($Y_I = 3.2$, Fig. 4a) and a β of 50° for pure mode *II* ($Y_{II} = 0.81$, Fig. 4b), as established by Ayatollahi and Aliha [32].

Conversely, the SCC specimen was used to analyze shear crack development under compressive loading. This cylindrical specimen,

Fig. 3. Testing apparatus and loading configurations for different tests in this study.

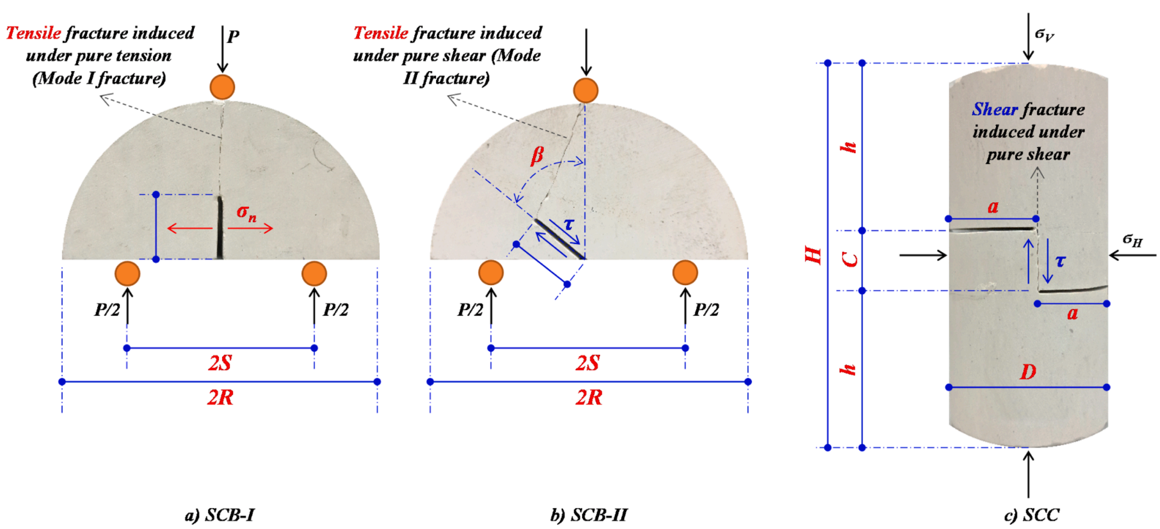

Fig. 4. Theoretical background of SCB and SCC methods, (a) SCB under pure tension, (b) SCB under pure shear, (c) SCC under pure shear.

with a standard height-to-diameter ratio (H/D) of 2, featured two parallel notches that created an intact rock bridge of length C (Fig. 4c). The analytical method involved applying a vertical compressive stress (σ_V) to induce shear stress concentration along this bridge, with an optional confining pressure (σ_H) to simulate in-situ conditions. The critical output of this analysis was the mode II fracture toughness ($K_{IIC\text{-}SCC}$), a material property defining resistance to shear cracking [33,34].

The determination of fracture toughness values was depended on the precise geometry of each specimen type. For the SCB analysis, the stress intensity factors under pure mode I and mode II were calculated using a standard equation (Eq. 1), which incorporated the measured critical load (P_{cr}) and the predetermined dimensionless factors for the selected configurations. For the SCC analysis, the value of $K_{IIC\text{-}SCC}$ was calculated using a separate established equation (Eq. 2), which included the applied stresses and critical geometric ratios of the specimen, notably H/D and C/H. This methodological separation enabled a focused investigation of tensile and shear fracture mechanisms under controlled and well-defined stress states.

$$K_{i-SCB} = \frac{P_{cr}}{2RT} Y_i \sqrt{\pi a} \ (i = I, II) \tag{1}$$

$$K_{IIC-SCC} = [2.3744(C/H) + 0.0192] \frac{P_{cr}\sqrt{\pi a}}{DC} \tag{2}$$

2.3. Integrating SCB and SCC methods with geological frameworks

Tensile and shear fractures induced through the SCB and SCC methods are highly significant and directly applicable to a wide range of geological and engineering contexts involving rocks in the Earth's crust. Tensile fractures, which occur under pure tension and are known as Mode I fractures, are prevalent in natural environments. These fractures are integral to many geological processes, such as rock fracturing in the Earth's crust, where they appear as joints resulting from tectonic stresses or cooling contractions—examples include columnar jointing in basalt (Fig. 5a). They also play a key role in hydraulic fracturing, where natural fluid pressures induce fractures similar to those created during reservoir stimulation (Fig. 5b, [35]). Exfoliation or sheeting joints in granite, caused by erosional unloading, is another natural manifestation of Mode I tensile fractures (Fig. 5c). Conversely, Mode II fractures induced by pure shear are less common but remain significant in certain scenarios. Among these, tensile fractures caused by pure shear are particularly notable; they often occur on the extensional side of faults. For example, pure Mode II tensile fractures can be generated by shear stress resulting

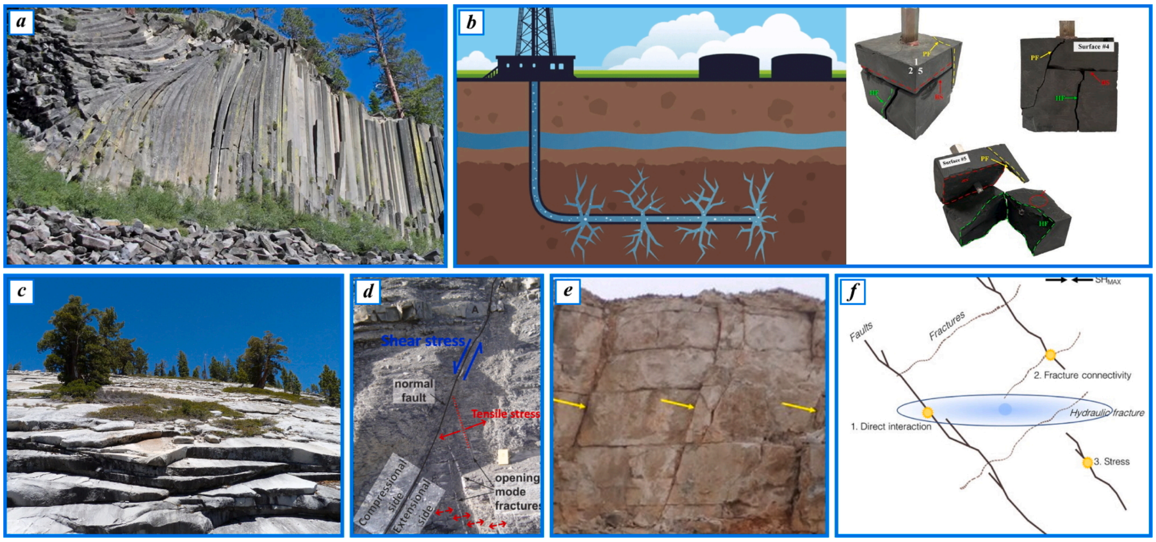

Fig. 5. Examples of natural fracture types that can be modeled using the SCB and SCC methods, (a) columnar jointing in basalt in Devils Postpile National Monument [37], (b) hydraulic fracturing [38], (c) granite sheeting joints, Yosemite National Park, California [39], (d) Vaca Muerta Formation, northwest Argentina [40], (e) Tectonic fractures in outcrops [41], (f) hydraulic fracture shear reactivation [36].

from fault slip on the extensional side of faults, such as those observed in the Vaca Muerta Formation in northwest Argentina (Fig. 5d). On the other hand, shear fractures induced in intact rock samples under uniaxial or triaxial compression using the SCC method effectively mimic natural shear failure processes and help to understand fault zone development and earthquake mechanics. These fractures are prominent along tectonic faults and occur in slope failures (Fig. 5e). Furthermore, hydraulic fracture shear reactivation—prompted by fluid injections such as fracking or geothermal stimulation—can reactivate pre-existing shear fractures, occasionally triggering induced seismicity (Fig. 5f, [36]).

3. Results

To initially explore the effect of thermal cycling on dolomite behavior, physical tests such as density and porosity were conducted both before and after thermal treatment. Porosity and density were determined using the water saturation technique, as described by Franklin, et al. [42]. This method calculates porosity from the difference between the saturated and dry weights of a rock specimen, based on the principle that the volume of water absorbed is equivalent to the sample's pore volume. The density and porosity results are presented in Fig. 6a, and detailed quantitative results for all parameters measured in this study are provided in Table 1. Overall, the findings indicate that with an increasing number of thermal cycles—from 0 to 50 and 100 cycles—there was a noticeable increase in density and a corresponding decrease in porosity. However, after 500 cycles, no significant changes in these parameters were observed compared to their values at 100 cycles. The observed increase in density and decrease in porosity imply an improvement in dolomite's behavior due to thermal cycling. This outcome contrasts with the typical expectations of weathering effects on rocks. Nonetheless, such behavior is not unusual in rock mechanics, as certain rock types exhibit enhanced properties when exposed to sustained or cyclic thermal conditions. These improvements can result from phenomena such as dehydration, thermal hardening, and the thermal expansion and contraction of dolomite grains. Such processes can promote the closure of primary pores and cracks, as further discussed later in Section 3.5.

It is important to note that this beneficial trend persists only up to a certain threshold. Beyond this point, the rock's behavior begins to deteriorate, primarily due to the loss of elastic properties in the grains and the accumulation of fatigue from cyclic thermal stress. Using a second-order polynomial fit, we determined that density and porosity

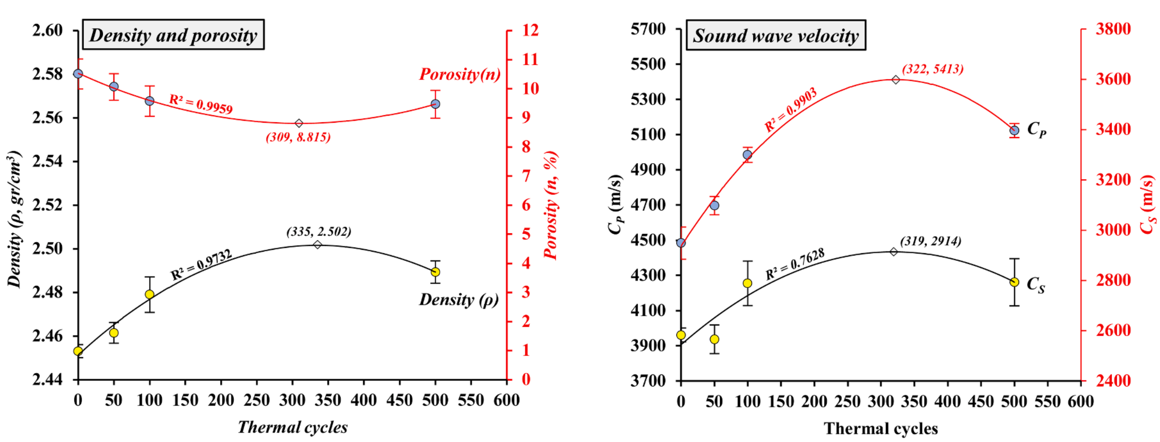

(a) (b)

Fig. 6. Thermal cycling effect on (a) density and porosity and (b) sound wave velocity.

Table 1
Data summary (Mean±SD/ Confidence level (95 %)).

Parameter	Unit	σ_3	Mean±SD/ Confidence level (95 %)			
			N=0	N=50	N=100	N=500
Density	gr/cm^3	–	2.453±0.003/0.003	2.461±0.004/0.005	2.479±0.008/0.009	2.489±0.005/0.005
Porosity	%	–	10.513±0.516/0.584	10.065±0.458/0.518	9.576±0.517/0.585	9.469±0.48/0.544
C_P	m/s	–	4483.6±92.18/39.425	4697.2±51.897/41.525	4985.2±43.276/32.059	5123.1±39.703/31.768
C_s	m/s	–	2582.8±27.769/11.877	2565.6±57.161/45.737	2788.3±88.741/65.739	2793±93.844/75.09
σ_t	MPa	–	5.318±0.507/0.574	5.447±0.789/0.893	5.998±0.671/0.759	6.372±0.433/0.49
σ_c	MPa	0	82±11.635/13.166	93.248±5.493/6.216	93.853±7.927/8.97	103.353±6.742/7.629
		3	110.393±7.015/7.938	114.011±6.435/7.282	124.574±9.029/10.218	134.735±10.528/11.914
		6	140.445±11.972/13.547	146.84±10.897/12.33	155.87±5.7/6.45	162.197±6.632/7.504
		12	170.899±10.605/12	185.166±12.397/14.028	192.828±8.589/9.719	210.982±13.443/15.212
τ	MPa	0	10.659±1.196/1.353	12.16±0.164/0.186	12.81±0.283/0.32	14.479±0.98/1.109
		3	17.658±1.538/1.74	21.846±0.885/1.002	27.265±2.712/3.069	34.328±3.027/3.426
		6	22.354±0.727/0.823	28.238±2.042/2.311	30.464±1.322/1.496	38.913±1.673/1.893
		12	41.984±2.599/2.941	46.974±2.673/3.024	53.102±1.263/1.429	62.548±5.278/5.973
K_{IC}	MPa mm$^{0.5}$	–	1.035±0.009/0.01	1.09±0.025/0.028	1.175±0.048/0.055	1.22±0.006/0.007
K_{IIC}	MPa mm$^{0.5}$	–	0.445±0.01/0.011	0.481±0.021/0.024	0.514±0.011/0.013	0.571±0.015/0.016
K_{IIS}	MPa mm$^{0.5}$	0	1.121±0.125/0.142	1.279±0.017/0.019	1.347±0.029/0.033	1.523±0.103/0.116
		3	1.857±0.161/0.183	2.298±0.093/0.105	2.868±0.285/0.322	3.611±0.318/0.36
		6	2.351±0.076/0.086	2.97±0.214/0.243	3.204±0.139/0.157	4.093±0.176/0.199
		12	4.416±0.273/0.309	4.941±0.281/0.318	5.586±0.132/0.15	6.579±0.555/0.628
E_t	GPa	–	30.023±2.224/2.517	32.232±1.477/1.671	35.197±1.008/1.141	36.541±1.932/2.186
E_I	GPa	–	2.22±0.202/0.229	2.733±0.251/0.284	3.283±0.175/0.198	3.416±0.225/0.255
E_{II}	GPa	–	4.853±0.35/0.396	5.12±0.301/0.341	5.371±0.29/0.328	5.641±0.381/0.431
E_c	GPa	0	22.212±2.948/3.336	24.76±2.431/2.751	27.572±1.581/1.789	29.415±2.888/3.268
		3	30.656±1.766/1.998	36.449±2.38/2.693	43.511±1.996/2.259	56.213±1.091/1.235
		6	30.919±1.957/2.215	38.239±3.839/4.345	46.692±1.592/1.801	58.396±3.076/3.48
		12	32.581±2.683/3.036	38.91±1.873/2.119	49.314±2.624/2.97	58.704±1.888/2.137
G	GPa	0	3.872±0.298/0.337	4.457±0.125/0.142	4.669±0.045/0.051	5.019±0.182/0.206
		3	4.195±0.136/0.154	4.51±0.188/0.213	5.324±0.308/0.349	5.872±0.137/0.155
		6	4.341±0.327/0.37	4.907±0.167/0.189	5.522±0.194/0.22	6.169±0.287/0.325
		12	4.906±0.489/0.553	5.59±0.142/0.16	5.939±0.022/0.025	6.464±0.172/0.194

improve with the number of thermal cycles up to thresholds of approximately 335 and 309 cycles, respectively. Beyond these thresholds, the properties begin to decline. The use of a second-order polynomial fit was chosen to capture the potential non-monotonic, two-phase behavior (increasing then decreasing, or vice versa) inherent in the material's response to thermal cycling. This approach provides a simple and effective model for identifying the presence of a turning point or optimum within the tested range.

To better understand the behavior of dolomite and assess the impact of thermal cycling on its physical properties, sound wave velocities—including both longitudinal and shear wave velocities—were measured before and after thermal cycling. The results are presented in Fig. 6b. Sound wave velocity is a sensitive indicator of rock integrity because it directly depends on the rock's structural composition, particularly the pore and fracture networks, which may be naturally occurring or induced by thermal cycling. As shown in Fig. 6, there is a strong correlation between sound wave velocity, porosity, and density. Specifically, a decrease in porosity corresponds to a significant increase in sound wave velocity, reaching a peak at approximately 320 cycles. Beyond this point, the sound wave velocity declines as porosity increases again.

3.1. Impact of thermal cycling on dolomite's mechanical strength

Fig. 7 illustrates the impact of thermal cycling on the mechanical strength of dolomite, including tensile strength, uniaxial and triaxial compressive strength, and shear strength of intact material. Among these properties, tensile strength is the most sensitive to thermal cycling, due to the development and propagation of microcracks induced by repeated heating and cooling. Thermal cycling leads to grain boundary weakening, void formation, and residual stress accumulation, which are particularly detrimental under tensile loading, as tensile stresses tend to open and extend micro-defects, while compressive stresses tend to close them. As shown in Fig. 7a, changes in tensile strength correlate strongly with variations in physical properties and ultrasonic wave velocities. Quantitatively, tensile strength increased by approximately 2.42 % after 50 cycles and 12.79 % after 100 cycles, reaching an estimated peak improvement of 24.28 % at N = 353 cycles. However, beyond this point, performance declined, with a 3.59 % reduction observed after 500 cycles relative to the peak value, suggesting the onset of thermal fatigue and microstructural degradation.

Regarding the effect of thermal cycles on the uniaxial and triaxial compressive strengths (Fig. 7b), a consistent trend is observed across different confining pressures (0, 3, 6, and 12 MPa), where the compressive strength initially increases by 31.95 %, 25.65 %, 20.9 %, and 27.5 % at threshold thermal cycles of 347, 367, 333, and 360, respectively, likely due to thermal-induced microcrack closure and densification of the material at moderate temperatures, but then decreases by 4.48 %, 2.86 %, 4.47 %, and 3.18 % after 500 thermal cycles, suggesting that prolonged thermal cycling eventually leads to cumulative damage, microcrack propagation, and structural degradation.

Regarding the effect of thermal cycles on shear strength (Fig. 7c), similar behavior can be observed, supporting the findings of this study. All parameters display consistent trends as the number of thermal cycles increases up to 500 cycles. If any measured parameter deviates from this pattern, it may indicate experimental error or an insufficient sample size, as the number of specimens may not be adequate to fully assess the material's response to thermal cycling. Since shear strength primarily depends on intergranular friction and shear of intact grains, the observed increase and subsequent decline in resistance after approximately 354–379 thermal cycles can be explained as follows: in the initial stage of thermal cycling (up to about 354–379 cycles), thermal expansion and contraction of the dolomite grains induce microstructural rearrangements. This includes the closure of micro-voids and improved grain interlocking, which temporarily enhances the material's mechanical stability and shear resistance. Beyond this threshold, however, the material begins to accumulate fatigue damage. Repeated thermal strains cause microcrack initiation and propagation, grain boundary weakening, and residual stress buildup. Over time, these micro-defects coalesce, weakening the rock's ability to resist shear forces. This

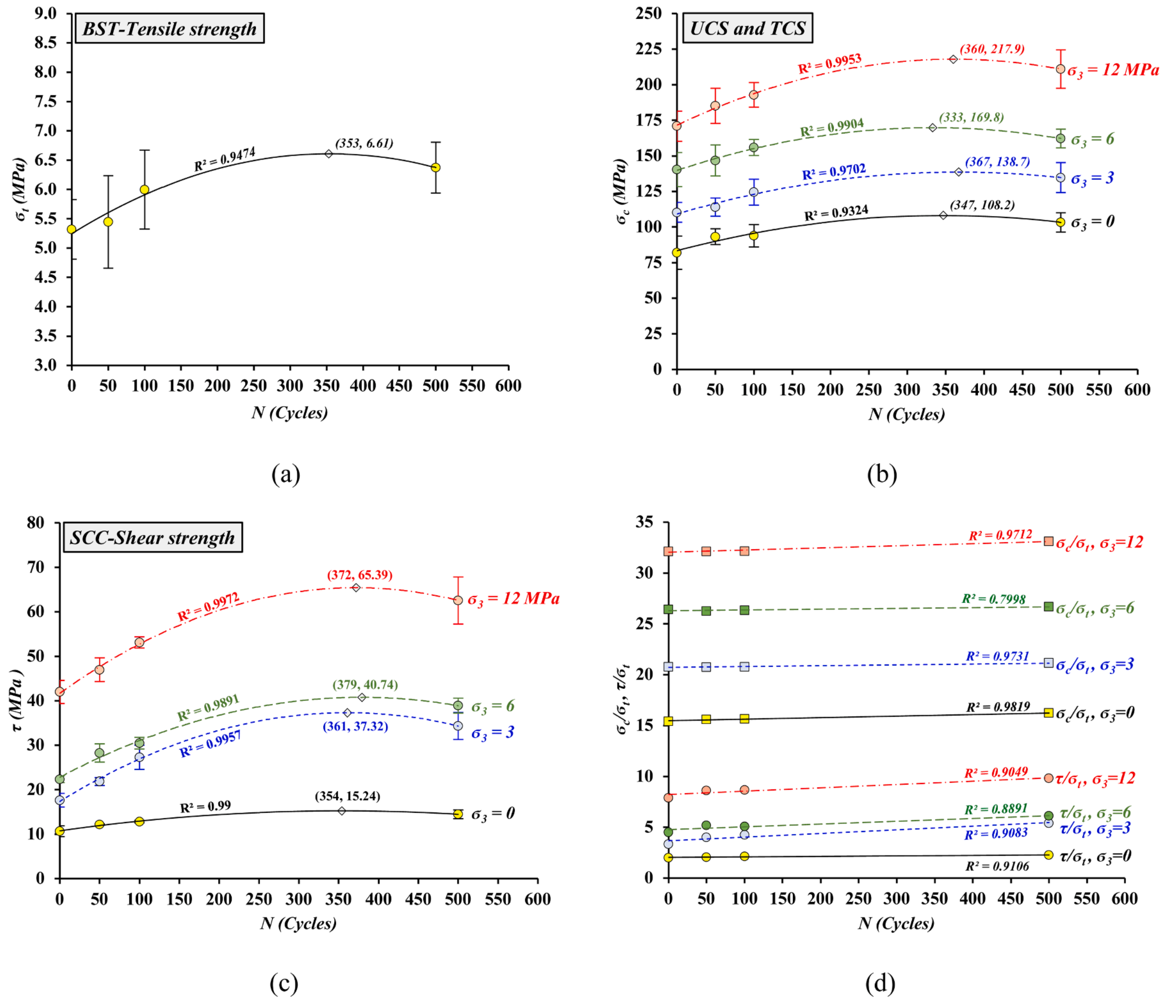

Fig. 7. Thermal cycling effect on dolomite's mechanical strength, (a) tensile strength, (b) uniaxial and triaxial compressive strength, (c) shear strength, (d) the evolution of the compressive-to-tensile (σ_c/σ_t) and shear-to-tensile (τ/σ_t) strength ratios.

transition marks the onset of degradation, as evidenced by the observed decrease in shear strength after 500 cycles, in contrast to the improvement noted between at 354 and379 cycles.

Fig. 7d illustrates the evolution of the compressive-to-tensile (σ_c/σ_t) and shear-to-tensile (τ/σ_t) strength ratios under varying confining pressures and thermal cycling conditions, showing that both ratios consistently increase with higher confining pressure—a predictable trend since confinement suppresses tensile failure while enhancing compressive and shear resistance by restricting dilation and microfracture propagation, thereby promoting frictional interlocking. Thermal cycling further amplifies this effect, with σ_c/σ_t and τ/σ_t ratios rising more noticeably at higher pressures (e.g., 12 MPa), indicating that prolonged thermal exposure modifies the rock's microstructure in a way that disproportionately strengthens compressive and shear resistance compared to tensile strength. By $N = 500$ cycles, the ratios peak, suggesting a cumulative thermal-induced strengthening effect that favors compressive and shear performance over tensile capacity, which has critical implications for rock stability in environments subject to cyclic thermal stresses.

The data scatter observed in some figures (e.g., Fig. 7a), where sample-to-sample fluctuations occasionally exceed the strength variation from cycling, is likely due to several experimental factors. These include inherent material heterogeneity and potential testing inaccuracies, such as slight loading misalignments or fabrication inconsistencies. Although the high correlation coefficient ($R > 0.9$) confirms a strong underlying trend, it does not account for this dispersion. Therefore, we performed a statistical analysis—calculating the standard deviation and confidence intervals at each cycle number—to quantify the uncertainty. This analysis strengthens the conclusions drawn from the experimental results, and its findings are summarized in Table 1.

3.2. Impact of thermal cycling on dolomite's fracture toughness

Fracture toughness is a critical parameter in rock mechanics, as it quantifies a rock's resistance to crack initiation and propagation under various loading modes—making it especially relevant for evaluating the stability of fractured geological structures subjected to environmental stresses. In this study, its significance is heightened by the inclusion of three distinct loading conditions—Mode I tensile (K_{IC}, SCB-I), Mode II tensile (K_{IIC}, SCB-II), and Mode *II* shear (K_{IIS}, SCC)—while also accounting for the influence of thermal fluctuations, which mimic natural weathering effects. As illustrated in Fig. 8, the impact of thermal cycling on fracture toughness is systematically explored across these modes, offering valuable insight into how dolomite's crack resistance evolves under cyclic thermal stress, and highlighting potential risks in thermally active geological settings. Fig. 8a shows that tensile fractures under pure tension are tougher than those under pure shear, with K_{IIC}/K_{IC} ranging from 2.14 to 2.32 for $N = 0$ to 500 thermal cycles. Both K_{IC} and K_{IIC} peaked at $N = 327$ and 367 cycles, respectively, mirroring the trend observed in other studied parameters. Fig. 8b also illustrates the influence of lateral pressure on the shear K_{IIS}. Fractures exhibit high sensitivity to lateral pressure, as it enhances friction along the shear planes,

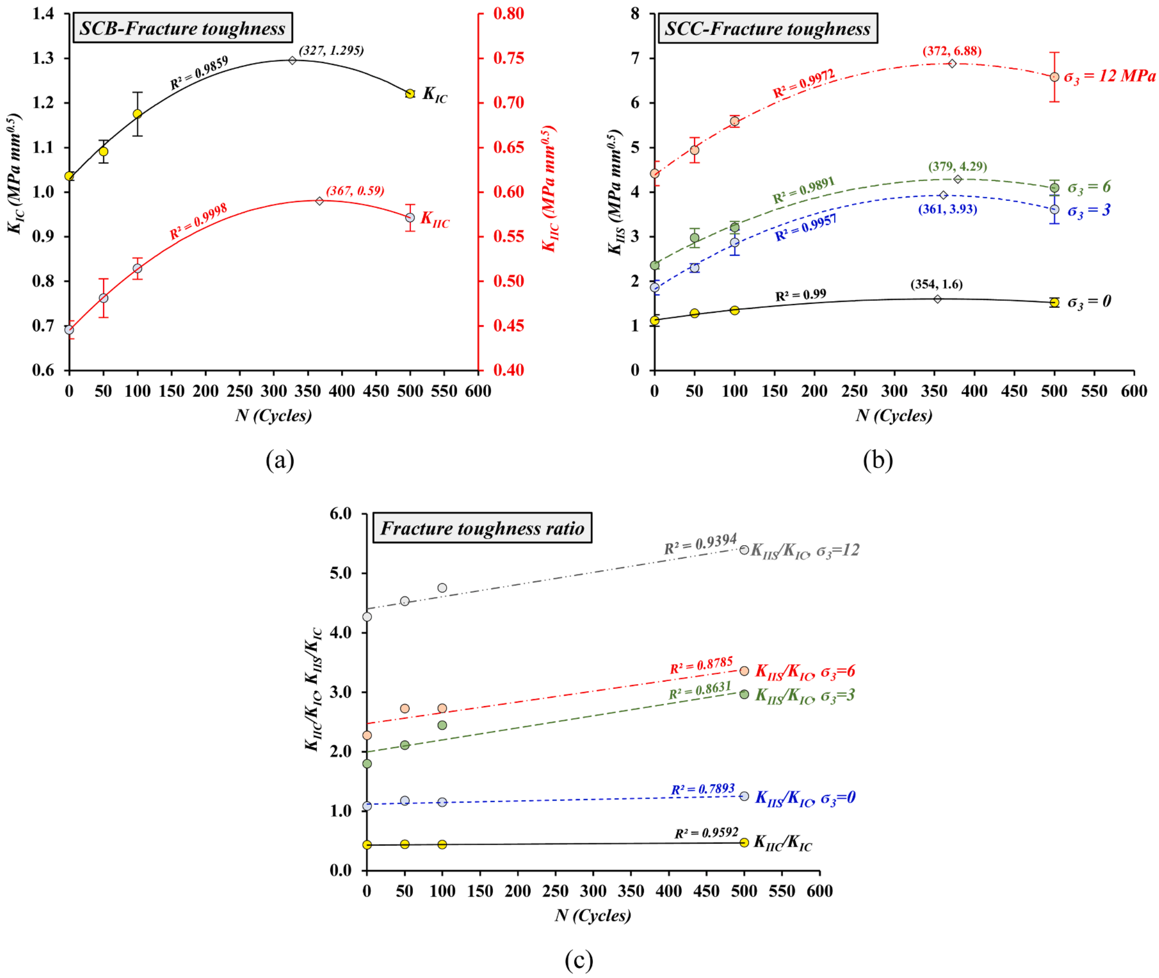

Fig. 8. Fracture toughness, (a) pure mode I and II tensile fracture toughness, (b) pure mode II shear fracture toughness, (c) fracture toughness ratio.

thereby increasing their resistance to shear. The results demonstrate a significant rise in peak shear fracture toughness—by 144.9 %, 167.3 %, and 329.1 %—under applied lateral pressures of 3, 6, and 12 MPa, respectively.

Fig. 8c illustrates the influence of thermal cycles on the fracture toughness ratio, a key parameter for assessing how thermal cycling alters fracture propagation behavior in rock. The provided data reveal that thermal cycling progressively increases both the Mode *II* tensile (K_{IIC}/K_{IC}) and Mode *II* shear (K_{IIS}/K_{IC}) fracture toughness ratios relative to Mode *I* tensile toughness, with K_{IIS}/K_{IC} showing a more pronounced enhancement (from 1.083 to 1.248) compared to K_{IIC}/K_{IC} (0.430 to 0.468), offering significant insights for rock mechanics and geological engineering. An increase in the number of thermal cycles (N) generally leads to an increase in both the K_{IIC}/K_{IC} and K_{IIS}/K_{IC}. Mechanically, a higher K_{IIS}/K_{IC} ratio indicates that a greater shear stress (relative to tensile stress) is required to propagate a fracture. Experimental evidence shows that thermal cycling preferentially enhances resistance to shear fracturing more than to tensile fracturing. Therefore, from a rock mechanics perspective, this suggests that for a rock subjected to frequent temperature variations, the stress conditions required for tensile failure will be met before those for shear failure in a wider range of scenarios. In other words, the rock may become relatively more prone to tensile fracturing as its resistance to shear fracturing is disproportionately increased. Geologically, this has profound implications for understanding rock mass stability, the evolution of rock discontinuities, and the initiation and propagation of fractures in engineering applications. For instance, in slope stability analysis, materials undergoing thermal cycling might exhibit altered failure mechanisms, potentially shifting from shear-dominated failures to more tensile-driven spalling or rockfall. This observed trend indicates that thermal fatigue can modify the inherent anisotropic fracture behavior of rocks, affecting joint development, fault reactivation, and the effectiveness of rock reinforcement strategies across various geological settings.

3.3. Impact of thermal cycling on elastic moduli

Elastic moduli, including tensile, compressive, and shear moduli, are fundamental parameters in rock mechanics and geological engineering because they quantify a rock's ability to deform under different types of stresses without permanent damage. Fig. 9 illustrates the effect of thermal cycling on elastic modulus under various loading conditions. Specifically, Fig. 9a shows the tensile modulus (E_t) from Brazilian splitting tests. Fig. 9b presents the tensile modulus measured at the notch tip of SCB specimens under pure mode *I* (E_I) and pure mode *II* (E_{II}) loading, derived from initial strain gauge data. Fig. 9c displays the compressive modulus from UCS and TCS specimens, while Fig. 9d shows the shear modulus (G) measured along the intact bridge between the notch tips in the SCC specimens. The results demonstrate strong agreement between the measured elastic moduli and other parameters in this study. Different elastic moduli of dolomite improve with an increasing number of thermal cycles, peaking within the threshold range of 310–386 cycles, after which they begin to decline. This enhancement in elastic moduli reflects greater resistance to external loads and an improved mechanical response, as evidenced by reduced deformations under stress. Specifically, higher elastic moduli correlate with increased load-bearing capacity and diminished deformation, a trend that aligns

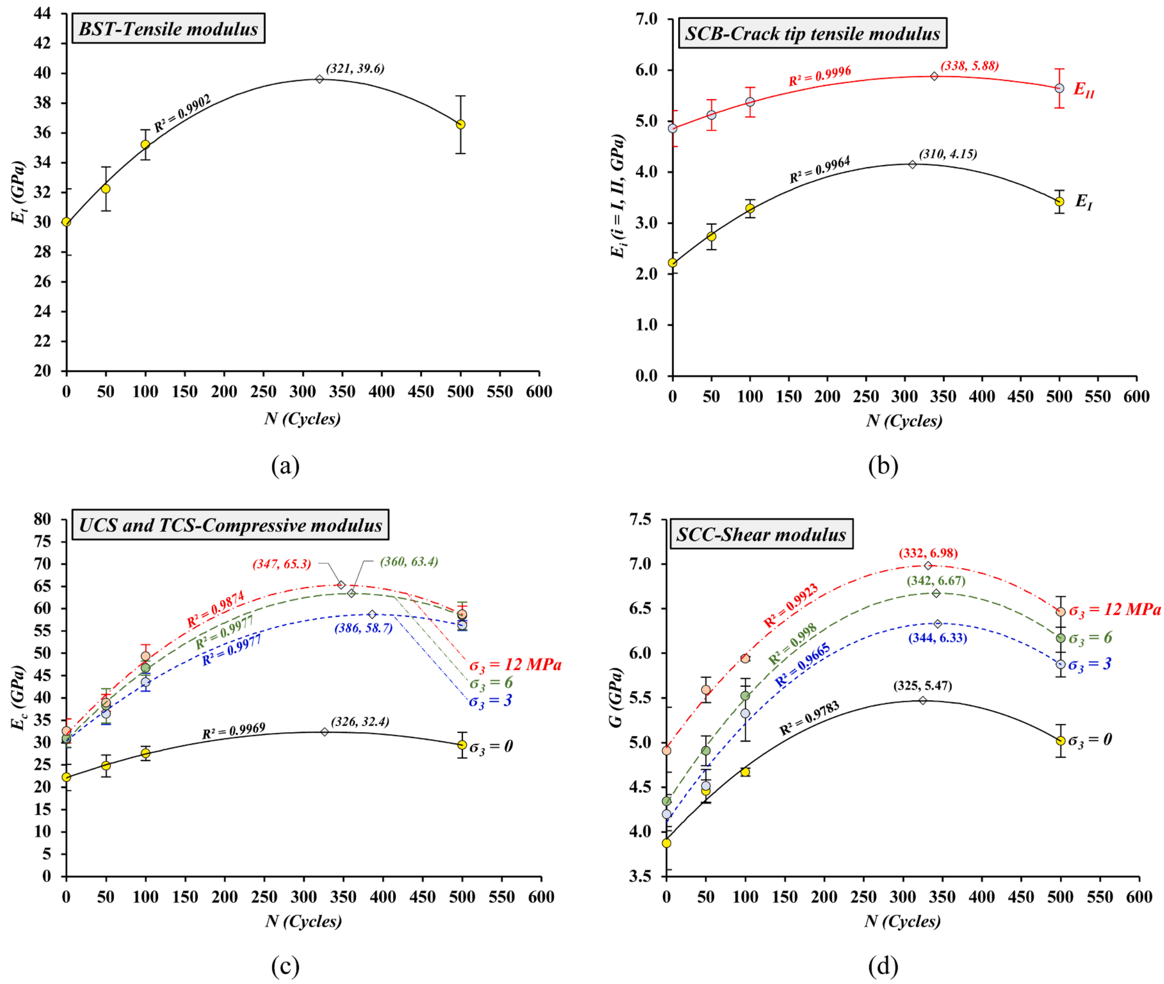

Fig. 9. Impact of thermal cycling on elastic moduli, (a) tensile modulus, (b) crack tip tensile modulus, (c) compressive modulus, and (d) shear modulus.

well with the observed effects of thermal cycling on dolomite's physical and strength properties. Furthermore, the Triaxial Compressive Strength (TCS) and Short Core in Compression (SCC) experiments—which account for lateral pressure effects—reveal a substantial increase in elastic modulus with rising confining pressure. At zero lateral pressure, the compressive modulus E_c ranges from 22.2 to 32.4 GPa, increasing to 32.6–65.3 GPa at a lateral pressure of 12 MPa. Similarly, the shear modulus G rises from an initial range of 3.9–5.5 GPa ($\sigma_3 = 0$ MPa) to 4.9–7.0 GPa at 12 MPa lateral pressure.

Comparing Fig. 9a and Fig. 9b, which illustrate the impact of thermal cycling on the tensile modulus of elasticity of intact (BST) and notches (SCB) specimens, it is evident that the intact BST specimens exhibit a substantially higher elastic modulus (E_t), specifically approximately 11.7 times greater than under pure Mode I (E_I) and 6.4 times greater than under pure Mode II (E_{II}) for the notched SCB specimens. This significant reduction in the tensile modulus of elasticity in the presence of notches underscores the profound influence of pre-existing discontinuities or fractures within the rock matrix. Such discontinuities act as stress concentrators, promoting localized deformation at their tips through mechanisms of crack opening (Mode *I*) or sliding (Mode *II*), thereby reducing the material's overall resistance to elastic deformation.

When comparing the tensile modulus of elasticity (E_t) with other elastic moduli (E_c and G), we observe that E_t is significantly higher—-even exceeding the compressive modulus measured under uniaxial stress conditions ($E_t \approx 1.3\ E_{c\text{-}U}$) and the shear modulus under varying lateral stresses (E_t = 5.7–7.8 G). This discrepancy arises from the inherently brittle nature of rocks under tensile loading. Unlike compression or shear, rocks subjected to tension exhibit minimal deformation before abrupt failure. This occurs because tensile stresses perpendicular to the primary fracture cause sudden separation of material grains, leading to immediate collapse. In contrast, rocks undergo greater deformation under compressive loads due to the closure of pre-existing pores and cracks, as well as sliding along crack surfaces before reaching their ultimate strength. Similarly, in SCC samples under shear stress, significant deformation occurs as pre-existing fracture surfaces slide before the formation of a critical shear plane, ultimately resulting in complete failure. These substantial deformations during compression and shear lead to a reduction in their respective elastic moduli compared to the tensile modulus (E_t).

3.4. Mineralogical and chemical changes induced by thermal fluctuations

The mineral and chemical composition of the tested dolomite was thoroughly analyzed before and after thermal cycling using three different methods. Initially, a thin section was prepared and observed under a 20X magnification microscope (Fig. 10a). While this examination offered some insight into the sample's structure, its mineralogical details remained somewhat limited, displaying only three distinct color variations: white, which may correspond to calcium-based minerals or quartz; gray, likely indicating clay or carbonate content; and black, representing empty spaces or pores within the sample. To obtain a more precise chemical composition, inductively coupled plasma-optical emission spectrometry (ICP-OES) was conducted (Fig. 10b). The results indicated that the rock was primarily composed of carbonates (45.05 %, lost upon ignition), lime (CaO, 42.33 %), and periclase (MgO, 12.13 %). To determine the phase composition of these chemical

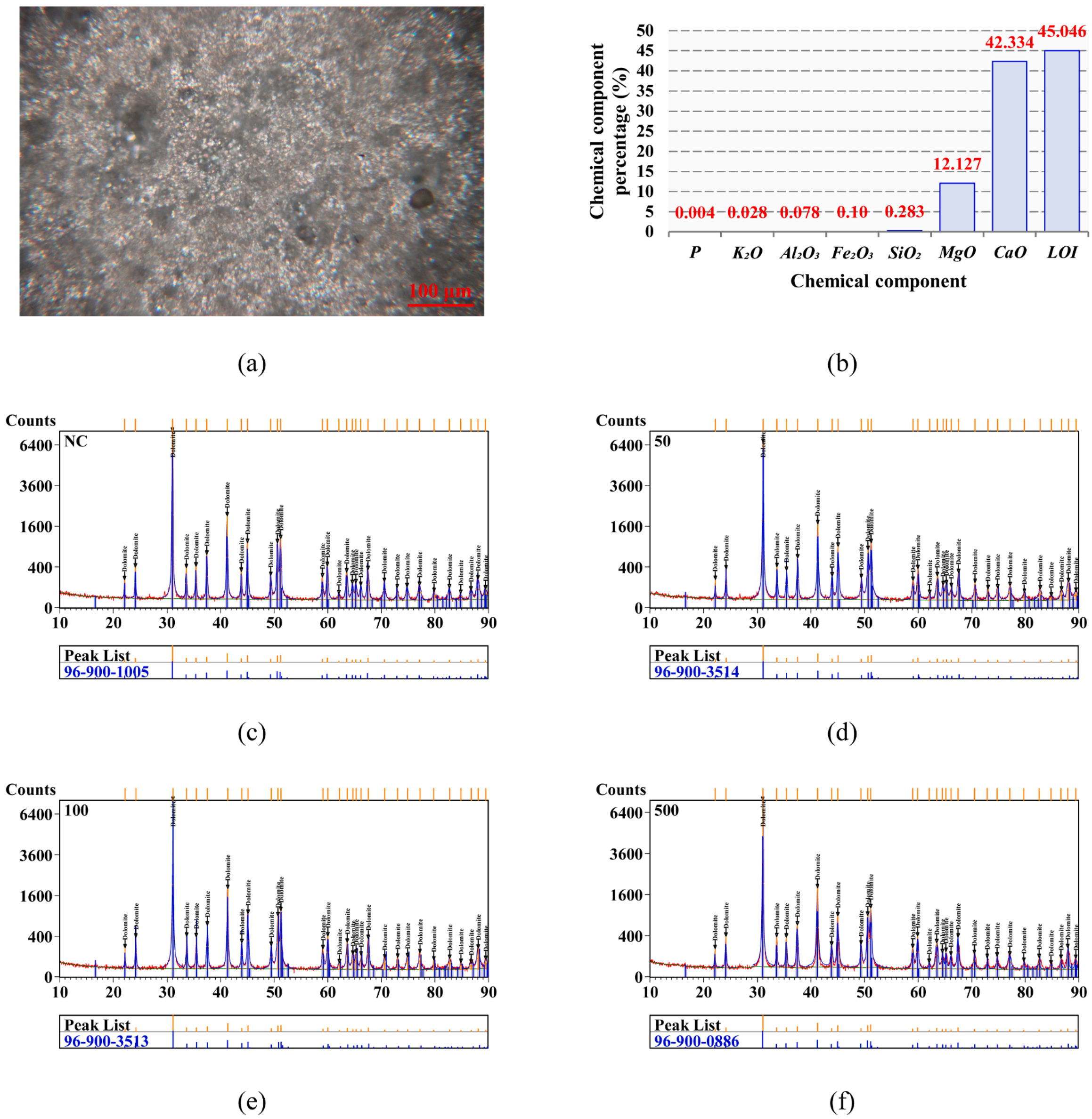

Fig. 10. Mineralogical and chemical composition of the tested dolomite before and after thermal cycling, (a) thin section at 20x magnification, (b) chemical composition, (c, d, e, and f) XRD pattern at 0, 50, 100, and 500 cycles, respectively.

constituents, X-ray diffraction (XRD) analysis was performed on the rock sample (Fig. 10c). The XRD pattern confirmed that dolomite ($CaMg(CO_3)_2$) is the dominant mineral phase.

The changes in the dolomite's behavior observed in this study cannot be attributed to alterations in its mineralogical or chemical composition. This is because the maximum temperature applied (60 °C) was well below the threshold required to induce phase transformations or chemical decomposition in this rock type. For instance, dolomite ($CaMg(CO_3)_2$) typically decomposes into calcite ($CaCO_3$), periclase (MgO), and carbon dioxide (CO_2) only at temperatures around 600 °C (see Eq. 2). At lower temperatures, dolomite retains its structural integrity under thermal exposure, as supported by previous studies [43,44]. To confirm this stability, XRD analysis was performed on the dolomite samples after 50, 100, and 500 thermal cycles. The results showed no evidence of phase changes or compositional decomposition (Fig. 10-d,e, and f), further confirming its thermal resilience under the tested conditions.

$$CaMg(CO_3)_2 \xrightarrow{600\ ^{\circ}C} CaCO_3 + MgO + CO_2 \tag{3}$$

3.5. Microstructural changes induced by thermal fluctuations

To investigate the microstructural evolution of dolomite induced by thermal cycling, Scanning Electron Microscopy (SEM) was employed with the primary purpose of observing the growth of thermal cracks and their subsequent effect on pre-existing voids. To ensure the analysis captured a representative sample of the bulk rock's response, thin sections were prepared from the cylindrical specimens used for compressive strength testing; these sections were taken perpendicular to the cylinder's axis to provide a symmetrical cross-sectional view of the core, a region that experiences a more uniform thermal history than the immediately exposed surface. These samples were examined both before and after exposure to thermal cycles at magnifications of 100×, 500×, and 2000×, facilitating detailed observation of microstructural features including grain boundaries, void formations, and crack development. This approach provided valuable insights into thermally driven alterations in the rock matrix, which correlate directly with changes in its mechanical behavior. Cracks and pores were examined at magnifications ranging from 100× to 2000×. The highest magnification (2000×)

proved most effective for distinguishing fracture types—whether intergranular or intragranular—as well as for assessing the influence of thermal cycles on the microstructure. At 2000× (Fig. 11a), all observed cracks were intergranular, occurring along grain boundaries, with no evidence of intragranular fractures within the grains. This indicates that thermal cycling did not alter the fracture mechanism.

The primary microstructural observation was a reduction in crack width as the number of thermal cycles increased. This trend is evident in Fig. 11e (after 500 cycles) compared to the control sample in Fig. 11b. Additionally, pore size decreased following 500 thermal cycles relative to untreated samples. To quantify these effects, the microstructural changes were analyzed by calculating surface porosity (pore area relative to total surface area), a key indicator of thermal cycling's impact on dolomite. As shown in Fig. 11f, surface porosity decreased by 72.3 % with increasing thermal cycles up to a threshold of 352 cycles, followed by a 46.9 % increase after 500 cycles. These trends align qualitatively with prior observations of thermal effects on rock porosity (Fig. 6a), providing a coherent explanation for the mechanical behavior of dolomite: initial improvement up to the threshold cycle count, followed by degradation beyond it.

The initial reduction in surface porosity observed up to 352 thermal cycles can be attributed to thermally induced compaction and crack-healing processes. Repeated heating and cooling likely promoted localized sintering and partial recrystallization along grain boundaries, which reduced pore volume and narrowed microcracks. Mismatches in thermal expansion among mineral grains generate localized compressive stresses, driving crack faces into closer contact and enhancing intergranular bonding. This microstructural densification provides a plausible mechanism for the concurrent improvement in mechanical properties during this stage. Beyond 352 cycles, accumulated thermal fatigue becomes the dominant mechanism, triggering the nucleation of new microcracks and the re-opening of previously healed fractures. The progressive increase in porosity (reaching 46.9 % after 500 cycles) signifies ongoing grain-boundary decohesion and microstructural deterioration, which erodes the mechanical performance gained earlier. The mechanical response of dolomite closely follows these porosity changes, underscoring the pivotal role of pore and crack networks in governing stress distribution.

In the initial regime, porosity reduction strengthened the rock by mitigating stress concentration points and enhancing load transfer across grain boundaries. This observation aligns with established behavior in brittle polycrystalline solids, where decreased porosity typically corresponds to increased strength and stiffness due to more efficient grain-to-grain load sharing and constrained crack propagation paths. In the subsequent regime, the porosity increase reintroduces internal stress concentrators, facilitating crack initiation and propagation under applied loading, thereby compromising cohesion and overall stiffness. The critical transition at 352 cycles marks a shift from advantageous thermal accommodation to irreversible damage accumulation, consistent with similar biphasic responses observed in thermally cycled geomaterials..

Mechanistically, the biphasic trend can be explained as the competition between short-term healing-assisted densification and long-term fatigue-driven degradation. Specifically, short-term mechanisms (≤ 352 cycles): transgranular and intergranular sintering, partial recrystallization, and grain-boundary bonding, which enhance solid contact, reduce pore connectivity, and decrease effective porosity. In contrast, long-term mechanisms (> 352 cycles) involve thermo-mechanical degradation, microcrack nucleation at grain boundaries, decohesion along interfaces, and porosity percolation effects that compromise load paths.

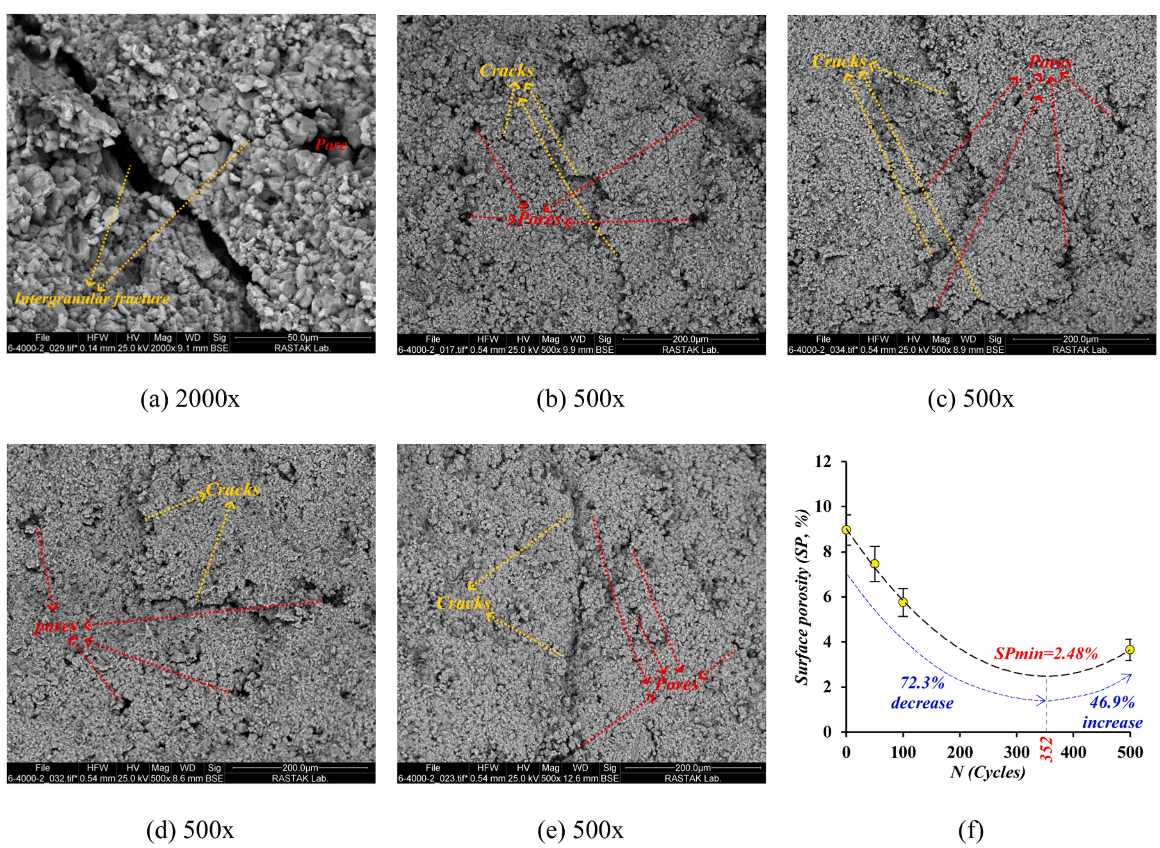

Fig. 11. Microstructural changes, (a) intergranular fractures and pores at 2000x magnification, (b, c, d, and e) SEM observation after N = 0, 50, 100, and 500 thermal cycles, respectively, (f) the effect of thermal cycles on surface porosity.

4. Discussion

Thermal cycling is a critical factor influencing the structural integrity and geomechanical behavior of geological formations within the Earth's crust, especially those rich in dolomite. Surface and shallow subsurface formations are continuously exposed to daily and seasonal temperature variations, which gradually weaken rock cohesion and provoke changes in physical and chemical properties. Over time, such fluctuations can degrade the durability of these formations, undermining their long-term stability. Furthermore, deeper formations—such as cavities and subsurface reservoirs extending to depths of approximately 2.5 km—are similarly affected by anthropogenic activities. The injection of drilling and working fluids during exploration or resource extraction introduces thermal anomalies that disrupt the natural temperature equilibrium. This artificial cooling, coupled with repeated heating during fluid circulation or geothermal gradient recovery, subjects dolomite-rich zones near boreholes and fracture networks to mechanical stress and mineralogical transformations. These processes can accelerate crack propagation, reduce rock strength, alter permeability, and compromise reservoir integrity—potentially leading to operational hazards, fluid leakage, or resource mismanagement. Therefore, understanding and quantifying the impact of cyclical thermal influence within this temperature range is essential for safe engineering design, sustainable extraction, and effective subsurface modeling.

The study revealed a non-monotonic enhancement in the mechanical behavior of the examined fresh dolomite rock with increasing thermal cycles, characterized by an initial improvement in properties up to a critical threshold of approximately 350 cycles, beyond which progressive deterioration commenced. This trajectory diverges from the conventional expectation of a consistent decline in rock stability under repeated thermal exposure and can be rigorously explained through the lens of fracture mechanics. The initial phase of mechanical enhancement is attributed to a process of microcrack tip blunting and localized compression. Volumetric expansion of dolomite grains during heating progressively encroaches upon existing pores and intergranular microcracks. From a fracture mechanics perspective, this expansion does not immediately drive crack propagation. Instead, it induces compressive stresses at the tips of pre-existing micro-flaws, effectively reducing their stress concentration factor. This blunting effect increases the energy required to reactivate these flaws as active cracks, thereby increasing the fracture toughness of the bulk material. The rock becomes more resilient, as more energy is needed to initiate and propagate new fractures.

However, this beneficial process contains the seeds of its own reversal. With continued cycling beyond the ~350-cycle threshold, the accumulated strain energy from repeated thermal expansion and contraction surpasses the energy dissipation capacity of the blunting mechanism. The failure mode shifts from beneficial crack-tip blunting to detrimental microcrack coalescence. New intra-granular thermal microcracks nucleate, and existing, now blunted, micro-cracks begin to link up. This creates a more connected and extensive fracture network, which significantly reduces the material's toughness. The propagation of a dominant macrocrack requires less energy as it can easily connect these pre-damaged zones, leading to the observed progressive deterioration in rock integrity. This transition is fundamentally a competition in energy dissipation mechanisms. In the initial stages, energy is dissipated through the grain expansion and crack-face friction (crack bridging). Beyond the threshold, energy is dissipated predominantly through the creation of new surface area (i.e., crack propagation), which is a sign of weakening. Furthermore, thermal cycling introduces rate-dependent effects and environmental weakening that further influence fracture behavior. Repeated heating and cooling induce thermal gradients and cyclic stress fields, which accelerate subcritical crack growth—a time-dependent fracture process sensitive to environmental conditions. In fresh dolomite, the lack of prior damage delays this process, allowing for temporary mechanical strengthening. However, once the material crosses the fatigue threshold, environmentally assisted cracking mechanisms—such as stress corrosion and thermally induced oxidation—begin to dominate, leading to accelerated degradation. Consequently, the behavior of thermally pre-conditioned dolomite (i.e., material starting beyond this threshold) would be fundamentally different. Such material would begin with a pre-existing, interconnected microcrack network, leading to diminished fracture toughness and resilience from the outset. This underscores that the documented response is specific to the initial condition of fresh dolomite and highlights the paramount importance of a rock's exposure history. A comprehensive assessment of the thermal response spectrum of geological formations must, therefore, be grounded in fracture mechanics principles that account for pre-existing damage state, microcrack interaction, and dominant energy dissipation pathways.

Building on previous studies investigating the effects of thermal cycling on rock behavior, Fig. 12 presents a detailed comparison between the results of our current study and those reported in the literature. The legend in this figure distinguishes between natural cooling (A) and sudden cooling in water (W) to clarify the experimental conditions of each study. Given the variation in the number of thermal cycles (N) across different studies, we normalized the thermal cycles to the maximum number of cycles ($N_{n_or} = N/N_{max}$) to facilitate direct comparison, ensuring that N_{n_or} always ranges between 0 and 1. Fig. 12a illustrates the influence of thermal cycling on S-wave velocity and tensile strength. Our results for S-wave velocity closely align with those reported by Zhang, et al. [19] for dolomitic marble subjected to gradual air cooling. Similarly, our tensile strength observations are consistent with the findings of Zhu, et al. [45] for granite, which exhibited a slight strength increase before $N_{n_or} = 0.2$. Fig. 12b further compares the effects of thermal cycling on different rock strength parameters, including peak shear strength (τ_p), compressive strength (σ_c), and dynamic compressive strength (σ_{cd}). Our data on compressive strength show strong agreement with Zhang, et al. [46], who studied dynamic compressive strength in granite under heating/air cooling cycles. Notably, Zhang, et al. [47] reported a marginal increase in τ_p for granite up to $N_{n_or} = 0.1$ under similar conditions. In contrast, Wang, et al. [48] observed a continuous increase in σ_c for sandstone subjected to heating/water cooling, while Jiang, et al. [49] documented a decreasing trend in τ_p for granite under heating/water cooling cycles. These variations highlight the critical role of cooling methods and rock composition in thermal cycling responses.

5. Conclusion

This study provides a comprehensive analysis of how moderate thermal cycling affects the tensile, compressive, and shear behavior of fresh, unweathered dolomite. Specimens underwent 50 (short), 100 (moderate), and 500 (long) thermal cycles between 20 °C and 60 °C before tensile, compressive, and shear testing. Additionally, compressive and shear tests were conducted under confining pressures of 3, 6, and 12 MPa to assess the influence of stress state on mechanical behavior. The effects of thermal cycling on dolomite's physical and mechanical properties are interpreted through changes in chemical composition, phase transformations, and microstructural evolution as a function of the number of cycles. The main conclusions are as follows:

- The thermo-mechanical response of carbonate rocks under cyclic heating significantly influences the long-term stability of slopes and excavations. Tests conducted on fresh dolomite subjected to 50–500 heating cycles between 20 and 60 °C reveal a two-stage behavior. Up to approximately 350 cycles, microcrack closure, grain-boundary recrystallization, and contact densification enhance strength, resulting in increases of 24.28 % in tensile strength, 31.95 % in unconfined compressive strength, and 42.96 % in shear strength. Beyond 350 cycles, fatigue effects surpass healing processes, causing strength reductions of 3.59 % (tensile), −4.48 % (UCS), and −4.98 % (shear) by 500 cycles. The results revealed that cyclic thermal stress progressively enhances both the Mode II tensile (K_{IIC}/K_{IC}) and Mode

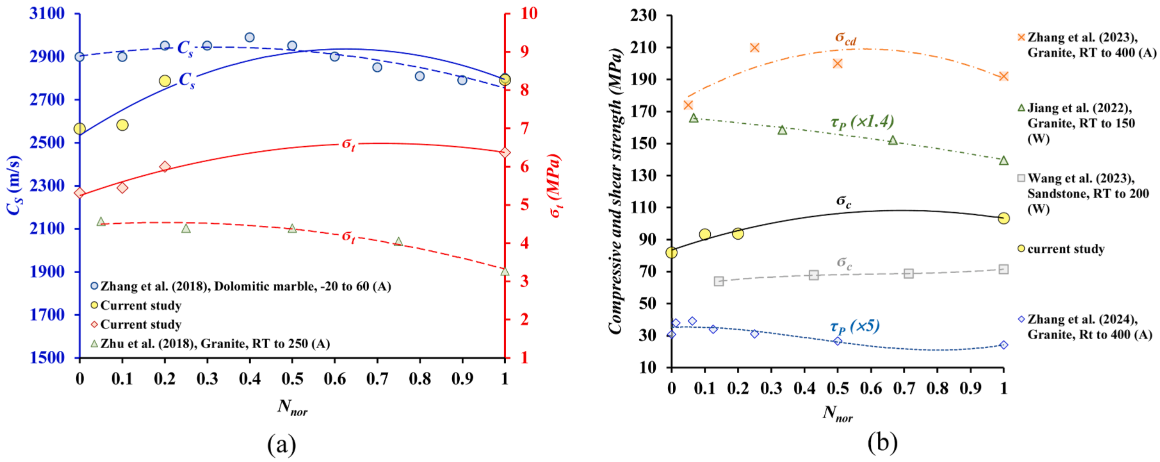

Fig. 12. Comparing the study's results with some previous literature, (a) shear wave velocity and tensile strength, (b) compressive and shear strength.

II shear (K_{IIS}/K_{IC}) fracture toughness ratios relative to Mode *I* tensile toughness (K_{IC}), indicating a significant evolution in the rock's anisotropic crack resistance under thermal fatigue, with the shear-dominated fracture toughness (K_{IIS}/K_{IC}) exhibiting a more pronounced increase (from 1.083 to 1.248) compared to the tensile-dominated Mode *II* (K_{IIC}/K_{IC}, increasing from 0.430 to 0.468).

- Thermal cycling tests on dolomite revealed a critical durability threshold, with all elastic moduli (tensile E_t, compressive E_c, and shear G) peaking between 310 and386 cycles. This peak indicates a temporary microstructural optimization phase, during which thermal stresses cause crack closure and mineral realignment, enhancing stiffness and load resistance before eventual degradation due to microcracking. Notably, the tensile modulus significantly exceeded the others, with $E_t \approx 1.3\, E_{c\text{-}U}$ and $E_t = 5.7\text{–}7.8\, G$. These findings are vital for predicting the long-term stability of rock masses in thermally dynamic environments.
- Thermal exposure up to 70 °C stabilized the chemical composition, however the microstructural void volume was highly sensitive to cycling. It decreased by 72.3 % after 352 cycles, then increased by 46.9 % at 500 cycles, a trend that strongly correlating with mechanical behavior. These transformations, reflected in density, porosity, and sound wave velocity, serve as key indicators of thermal fatigue. The fluctuations underscore the critical role of microstructural evolution, where accumulating cycles drive fatigue cracks and alter the internal architecture, ultimately governing the material's overall mechanical performance.

Limitations and future directions

This study, while providing fundamental insights into the thermo-mechanical behavior of dolomite, is subject to several limitations that outline avenues for future research. The conclusions are derived from laboratory-scale tests on small, intact specimens, which may not fully capture the large-scale, heterogeneous nature of in-situ rock masses containing joints, fractures, and lithological variations. Furthermore, the material properties were treated deterministically, and the investigation was limited to dry conditions; a saturated state, representative of many subsurface environments, would likely alter the response due to pore pressure effects and potential chemical interactions. Finally, the loading conditions were simplified to pure Mode I, II, and shear, whereas real-world applications often involve complex mixed-mode loading scenarios.

Future work should focus on bridging the gap between laboratory observations and field-scale validation. Investigations under mixed-mode loading and fatigue crack growth regimes are essential to develop more comprehensive failure criteria for thermally cycled rock. To enhance the practical relevance of these findings, experiments should be conducted under conditions that more closely mimic critical geo-engineering environments. This includes applying higher confining pressures (e.g., >12 MPa), simulating deeper geological settings, and employing cycle temperatures exceeding 60 °C to assess performance in more intense thermal operations such as enhanced geothermal systems. In addition, the number of thermal cycles considered in this study is typically limited to a maximum of 500. While a good starting point, this constraint might not fully reveal the long-term degradation mechanisms or fatigue properties of dolomite subjected to prolonged thermal fluctuations. Therefore, an important focus for future research is to greatly increase the number of thermal cycles beyond 500. Additionally, performing intermediate tests, specifically around the 350-cycle mark, is recommended to experimentally identify the threshold point at which dolomite behavior or performance begins to substantially alter or deteriorate. This approach would allow for the precise determination of critical limits, leading to improved durability and reliability assessments for underground structures. Ultimately, in-situ validation through controlled field trials or monitoring of actual engineering structures is crucial for calibrating laboratory models and confirming the long-term predictive power of the proposed mechanisms.

CRediT authorship contribution statement

Abdel Kareem Alzo'ubi: Writing – review & editing, Writing – original draft, Visualization, Validation, Supervision, Software, Resources, Project administration, Methodology, Investigation, Funding acquisition, Formal analysis, Data curation, Conceptualization. **Mahmoud Alneasan:** Writing – review & editing, Writing – original draft, Visualization, Validation, Software, Resources, Methodology, Investigation, Formal analysis, Data curation, Conceptualization.

Declaration of competing interest

The authors whose names are listed immediately below certify that they have NO affiliations with or involvement in any organization or entity with any financial interest (such as honoraria; educational grants; participation in speakers' bureaus; membership, employment, consultancies, stock ownership, or other equity interest; and expert testimony or patent-licensing arrangements), or non-financial interest (such as personal or professional relationships, affiliations, knowledge or beliefs) in the subject matter or materials discussed in this manuscript.

The authors whose names are listed immediately below report the following details of affiliation or involvement in an organization or entity with a financial or non-financial interest in the subject matter or materials discussed in this manuscript. Please specify the nature of the conflict on a separate sheet of paper if the space below is inadequate.

Acknowledgment

We thank the ORSP at Abu Dhabi University for funding this project (19300856)

Data availability

Data will be made available on request.

References

[1] L.C. Resio, Dolomite thermal behaviour: a short review, Phys. Chem. Min. 51 (2024) 19.
[2] Y. Zhang, X. Ta, S. Qin, Effect of heat treatment on physico-mechanical behaviour of a natural building stone: Laizhou dolomite marble, J. Build. Eng. 47 (2022) 103885.
[3] Y.-L. Chen, Y.-G. Pan, X. Du, L. Shao, W.-C. Guan, Y.-F. Tang, G.-L. Liu, R. Azzam, T.M. Fernandez-Steeger, Multi-scale damage experiments and constitutive studies of rocks with different mineral compositions under high temperature effects, Results. Eng. 27 (2025) 105734.
[4] B. Qiu, Z. Wang, X. Zhao, L.F. Fan, Triaxial compressive failure of thermally damaged granite following low- and high-cycle fatigue loading, Results. Eng. 26 (2025) 105142.
[5] A.K. Alzo'ubi, M. Alneasan, F. Ibrahim, The mechanical behavior of mudstone under coupling effect of temperature and confining pressure: A comprehensive investigation, Rock. Mech. Rock. Eng. 57 (2024) 2325–2338.
[6] H. Zhou, Z. Liu, F. Liu, J. Shao, G. Li, Anisotropic strength, deformation and failure of gneiss granite under high stress and temperature coupled true triaxial compression, J. Rock Mech. Geotech. Eng. 16 (2024) 860–876.
[7] X. Li, B. Yan, Q. Wang, Z. Hong, Y. Zhang, C. He, Wave velocity evolution law and mechanical index attenuation model of limestone under different freeze-thaw cycles, Results. Eng. 26 (2025) 105216.
[8] P. Zhang, C. Wang, Z. Gao, Z. Wang, C. Zhou, F. Wang, Combined effects of high temperature and lithology on the tensile mechanical damage and fracture surface morphology of reservoir rocks, Bull. Eng. Geol. Env. 83 (2024) 226.
[9] L.N.Y. Wong, Y. Zhang, X. Cui, Z. Wu, Thermal effect on rock strength: strengthening-weakening transition explored by grain-based model, Acta Geotech. 19 (2024) 3321–3336.
[10] M. Alneasan, A.K. Alzo'ubi, F. Ibrahim, A comparison between conventional and generalized fracture criteria to predict fracture parameters in clay rich rocks (Mudstone) under temperature effect, Constr. Build. Mater. 416 (2024) 135168.
[11] N. Shen, L. Wang, X. Li, The effect of temperature on injection-induced shear slip of laboratory faults in sandstone, Acta Geotech. (2024).
[12] M. Alneasan, A.K. Alzo'ubi, Extensive experimental investigation on the effect of thermal treatment and lateral pressure on the shear behavior of intact mudstone, Sci. Rep. 13 (2023) 6820.
[13] P. Wang, C. Wang, G. Wang, Y. Jiang, F. Xu, Experiment study on shear behavior and properties of granite fractures under real-time high-temperature conditions, Geomech. Energy Environ. 38 (2024) 100539.
[14] G. Feng, X. Wang, Y. Kang, Z. Zhang, Effect of thermal cycling-dependent cracks on physical and mechanical properties of granite for enhanced geothermal system, Int. J. Rock Mech. Min. 134 (2020) 104476.
[15] L.N.Y. Wong, T.Y. Guo, Z. Wu, X. Xiao, How do thermally induced microcracks alter microcracking mechanisms in Hong Kong granite? Eng. Geol. 292 (2021) 106268.
[16] J. Jin, D. Wang, J. Lu, L. Yin, H. Xiao, J. Li, Effects of dry–wet and freeze–thaw cycles on the mechanical properties and microstructure of quartz schist, Results. Eng. 27 (2025) 105770.
[17] S.N. Longinos, P. Skrzypacz, R. Hazlett, Cryofracturing effectiveness using liquid nitrogen on granite: fracture toughness and Brazilian tests following freezing-thawing cycle, Results. Eng. 21 (2024) 101895.
[18] M. Hajpál, Changes in sandstones of historical monuments exposed to fire or high temperature, Fire Technol. 38 (2002) 373–382.
[19] Z.J. Zhang, J.B. Liu, B. Li, X.G. Yang, Thermally induced deterioration behaviour of two dolomitic marbles under heating–cooling cycles, R. Soc. Open. Sci. 5 (2018) 180779.
[20] G. Rong, J. Peng, M. Cai, M. Yao, C. Zhou, S. Sha, Experimental investigation of thermal cycling effect on physical and mechanical properties of bedrocks in geothermal fields, Appl. Therm. Eng. 141 (2018) 174–185.
[21] C. Mo, J. Zhao, D. Zhang, Real-time measurement of mechanical behavior of granite during heating–Cooling cycle: A mineralogical perspective, Rock. Mech. Rock. Eng. 55 (2022) 4403–4422.
[22] C.J. Villarraga, M. Gasc Barbier, J. Vaunat, J. Darrozes, The effect of thermal cycles on limestone mechanical degradation, Int. J. Rock Mech. Min. 109 (2018) 115–123.
[23] T. Voake, A. Nermoen, C. Ravnås, R.I. Korsnes, I.L. Fabricius, Influence of temperature cycling and pore fluid on tensile strength of chalk, J. Rock Mech. Geotech. Eng. 11 (2019) 277–288.
[24] Y. Cui, L. Xue, M. Zhai, C. Xu, F. Bu, L. Wan, Experimental investigation on the influence on mechanical properties and acoustic emission characteristics of granite after heating and water-cooling cycles, Geomech. Geophys. Geo. Energy Geo. Resour. 9 (2023) 88.
[25] W. Liu, L. Zhang, N. Luo, Elastic modulus evolution of rocks under heating–cooling cycles, Sci. Rep. 10 (2020) 13835.
[26] S. Ge, C. Wu, C. He, Y. Wang, D. Chen, B. Shi, Thermal damage of high-temperature sandstone subjected to cooling shock and its effect on capturing acoustic emission signals during fracture, Eng. Fail. Anal. 145 (2023) 107003.
[27] A. Mosaddegh, A. Fahimifar, P. Najafipour, Influence of thermal and cooling cycles on the mechanical properties of building stones with carbonate texture, Geothermics 130 (2025) 103330.
[28] J. Hu, H. Xie, M. Gao, C. Li, Q. Sun, Damage mechanism and heat transfer characteristics of limestone after thermal shock cycle treatments based on geothermal development, Int. J. Rock Mech. Min. 160 (2022) 105269.
[29] M. Gasc-Barbier, V. Merrien-Soukatchoff, V. Krzewinski, P. Azemard, J.-L. Genois, Assessment of the influence of natural thermal cycles on dolomitic limestone rock columns: A 10-year monitoring study, Geomorphology 464 (2024) 109353.
[30] A.K. Alzo'ubi, Stability of a rock slope susceptible to seasonal movements, GEOMATE J. 6 (2014) 800–805.
[31] D. Zhu, H. Jing, Q. Yin, S. Ding, J. Zhang, Mechanical characteristics of granite after heating and water-cooling cycles, Rock. Mech. Rock. Eng. 53 (2020) 2015–2025.
[32] M.R. Ayatollahi, M.R.M. Aliha, Wide range data for crack tip parameters in two disc-type specimens under mixed mode loading, Comput. Mater. Sci. 38 (2007) 660–670.
[33] Y. Xu, W. Yao, G. Zhao, K. Xia, Evaluation of the short core in compression (SCC) method for measuring mode II fracture toughness of rocks, Eng. Fract. Mech. 224 (2020) 106747.
[34] M. Alneasan, A.K. Alzo'ubi, N. Okasha, A comprehensive study for the effect of sample geometry and lateral pressure on shear fractures using the short core in compression (SCC) method, Eur. J. Mech. A Solids 100 (2023) 104988.
[35] H. Qu, Z. Li, C. Li, X. Liu, Z. Zeng, Y. Xu, Y. Liu, Experimental study of fracture initiation and morphology in low-brittle shales with bedding planes subjected to LN fracturing, Rock. Mech. Rock. Eng. 56 (2023) 6299–6319.
[36] N. Igonin, J.P. Verdon, J.M. Kendall, D.W. Eaton, Large-scale fracture systems are permeable pathways for fault activation during hydraulic fracturing, J. Geophys. Res. Solid 126 (2021) e2020JB020311.
[37] Vertical columns of volcanic rock at Devils Postpile National Monument. https://www.usgs.gov/volcanoes/long-valley-caldera/science/vertical-columns-volcanic-rock-devils-postpile-national, 2023.
[38] Hydraulic Fracturing: Techniques, Benefits, and Impact. https://www.petrosync.com/blog/hydraulic-fracturing/, 2025.
[39] Granite sheeting joints. https://www.flickr.com/photos/35142635@N05/7545021642/, 2012.
[40] J.F. Gale, S.E. Laubach, J.E. Olson, P. Eichhubl, A. Fall, Natural fractures in shale: A review and new observationsNatural Fractures in shale: A review and new observations, Am. Assoc. Pet. Geol. Bull. 98 (2014) 2165–2216.
[41] G. Liu, L. Zeng, C. Han, M. Ostadhassan, W. Lyu, Q. Wang, J. Zhu, F. Hou, Natural fractures in carbonate basement reservoirs of the Jizhong Sub-Basin, Bohai Bay Basin, China: key aspects favoring oil production, Energies 13 (2020) 4635.
[42] J. Franklin, S. ZONGQI, B. Atkinson, P. Meredith, F. Rummel, W. Mueller, Y. Nishimatsu, H. Takahahsi, L. Costin, A. Ingraffea, Suggested methods for determining the fracture toughness of rock, Int. J. Rock Mech. Min. Geomech. Abstr. 25 (1988).
[43] M.J. Trindade, M. Dias, J. Coroado, F. Rocha, Mineralogical transformations of calcareous rich clays with firing: a comparative study between calcite and dolomite rich clays from Algarve, Portugal, Appl. Clay. Sci. 42 (2009) 345–355.
[44] M. Olszak-Humienik, M. Jablonski, Thermal behavior of natural dolomite, J. Therm. Anal. Calorim. 119 (2015) 2239–2248.
[45] D. Zhu, H. Jing, Q. Yin, G. Han, Experimental study on the damage of granite by acoustic emission after cyclic heating and cooling with circulating water, Processes 6 (2018) 101.
[46] H. Zhang, L. Huang, X. Li, X. Hu, Y. Wu, Study on the evolution of physical parameters and dynamic compression mechanical properties of granite after different heating and cooling cycles, Materials 16 (2023) 2300.
[47] G.H. Zhang, Z.Y. Han, S.L. Li, L.Z. Dan, F. Xiong, Z.C. Tang, Changes in shear properties of granite fractures subjected to cyclic heating and air-cooling treatments, J. Rock Mech. Geotech. Eng. 16 (2024) 4925–4943.
[48] W. Wang, L. Hong, X. Cao, X. Lu, F. Wang, T. Zhang, W. Zhu, Experimental study of the mechanical and acoustic emission characteristics of sandstone by using high-temperature water-cooling cycles, Sustainability 15 (2023) 13358.
[49] Z. Jiang, Q. Yin, J. Wu, Q. Zhu, M. Li, H. Su, H. Jing, The effect of cyclic heating and cooling on mechanical and deformation responses of granites under preset angle shearing, Env. Earth Sci. 82 (2022) 29.